


Article

Computational Study of Some 4'-Aryl-1,2,4-triazol-1-ium-4-R₂-phenacylid Derivatives in Vacuum and Dimethylformamide

Nicoleta Melniciuc Puica ^{1,*}, Dan-Gheorghe Dimitriu ^{2,*} , Gabriela Apreotesei ³, Ana Cezarina Moroşanu ^{2,4} and Dana-Ortansa Dorohoi ²

¹ Faculty of Orthodox Theology, Alexandru Ioan Cuza University, 9 Closca Str., RO-700066 Iasi, Romania

² Faculty of Physics, Alexandru Ioan Cuza University, 11 Carol I Blvd., RO-700506 Iasi, Romania

³ Faculty of Machine Manufacturing and Industrial Management, Gheorghe Asachi Technical University, RO-700050 Iasi, Romania

⁴ Department of Physics, Petru Rareş National College, 4 Stefan cel Mare Street, RO-600121 Piatra Neamt, Romania

* Correspondence: nicoleta.melniciuc@uaic.ro (N.M.P.); dimitriu@uaic.ro (D.-G.D.)

Abstract: Four carbanion monosubstituted 4'-aryl-1,2,4-triazol-1-ium-4-R₂-phenacylids, used as precursors in obtaining new heterocyclic compounds, and their corresponding derivatives belonging to the C_{2v} point group of symmetry were studied by computational means in dimethylformamide (DMF) solutions compared with their isolated state. The changes in the computed parameters induced by the solvent compared with those of the isolated molecules were analyzed in this paper. The charge distribution and the molecular energies in the HOMO and LUMO, the electronic states responsible for the visible absorption band of 4'-aryl-1,2,4-triazol-1-ium-4-R₂-phenacylids, in their isolated state and in solutions achieved in DMF were computed and compared with the visible electronic absorption spectra. The molecular descriptors of the studied compounds were computed, and the higher reactivity of the carbanion monosubstituted 4'-aryl-1,2,4-triazol-1-ium-4-R₂-phenacylids compared with symmetric derivatives was established. The obtained results can help researchers to obtain new heterocycles with applications in the drug industry.

Keywords: 1,2,4-triazol-1-ium-phenacylids; computed physical-chemical parameters; molecular descriptors; visible electronic absorption spectra



Citation: Melniciuc Puica, N.; Dimitriu, D.-G.; Apreotesei, G.; Moroşanu, A.C.; Dorohoi, D.-O. Computational Study of Some 4'-Aryl-1,2,4-triazol-1-ium-4-R₂-phenacylid Derivatives in Vacuum and Dimethylformamide. *Symmetry* **2022**, *14*, 2099. <https://doi.org/10.3390/sym14102099>

Academic Editors: Cheng Zhan and Jan Cz. Dobrowolski

Received: 24 August 2022

Accepted: 2 October 2022

Published: 8 October 2022

Publisher's Note: MDPI stays neutral with regard to jurisdictional claims in published maps and institutional affiliations.



Copyright: © 2022 by the authors. Licensee MDPI, Basel, Switzerland. This article is an open access article distributed under the terms and conditions of the Creative Commons Attribution (CC BY) license (<https://creativecommons.org/licenses/by/4.0/>).

1. Introduction

1,2,4-Triazolium derivatives are substances used as precursors in obtaining new heterocyclic compounds with multiple applications. Due to the high importance of triazolium derivatives, some reviews have recently been published in this field [1,2]. The industrial and pharmacological applications, clinical implications and efficiency and fabrication costs of triazolium derivatives were discussed in these reports. The triazolium derivatives were tested against some bacteria and pathological fungi [3,4] providing good or moderate activity against them. Most 1,2,4-triazolium derivatives are known for their antitumoral, analgesic, anti-inflammatory, psychoactive, diuretic or anti-HIV actions [1–4].

A series of triazole derivatives with medical applications have recently been studied and published [5–8]. For example, N-1-substituted-1,2,4-triazolium-based ionic liquids were recognized, by specific means (UV, NMR, fluorescence lifetime control, circular dichroism), as being compatible media for hemoglobin stability [8]. Mesophases were obtained from some 1,2,4-triazolium derivatives bearing a perfluoroalkyl chain [9]. The synthesis of some β -carbonyl compounds was realized based on 1-phenyl-1,2,4-triazolium methanesulfonate as an ionic liquid organocatalyst at room temperature [10]. The reduction of various aldehydes and ketones was realized by boron hydride in the presence of 1-hexyl-1,2,4-triazolium methanesulfonate and 1-hexyl-1,2,4-triazolium trifluoroacetate [11].

1,2,4-Triazol-1-ium ylids are used as precursors in different industrial activities [12,13], especially in the pharmacological industry [14–16], in which more than half of known drugs contain at least one heterocycle compound [17].

1,2,4-Triazol-1-ium phenacylids are stable, dipolar, colored cycloimmonium ylids [18–20] with separated charges on the ylid bond, N^+-C^- . The positively charged nitrogen belongs to a five-membered heterocycle containing three nitrogen atoms. The negative carbon of the ylid bond can be mono- or bisubstituted if it is bonded with a hydrogen atom and a highly electronegative atomic group or with two electronegative atomic groups, respectively. The stability of cycloimmonium phenacylids is assured by the electrostatic interactions between the charged parts of the molecule, by the charge delocalization on the carbanion and heterocycle and also by the resonant structures [18]. Due to their high reactivity, the carbanion monosubstituted 1,2,4-triazolium phenacylids are used to obtain new drugs based on heterocyclic structures.

A series of important applications of ionic liquids based on the 1,2,4-triazolium derivatives with special properties such as low vapor pressure, liquidity over a wide temperature range, high thermal stability, ionic conductivity and the ability to dissolve a wide range of substances have been studied recently [21]. Tankov and Yankova [22] evidenced (using the density functional theory) the large electropositive potential of the 1,2,4-triazolium ring and tested the catalytic reactivity of 4-amino-1H-1,2,4-triazolium nitrate in the reaction of acid acetic esterification at different temperatures. The density functional theory was also applied in studies regarding the acidity of 1,2,3-triazolium ions [23].

Computational studies of some aryl-1,2,4-triazol-1-ium ylids were performed in some hydroxyl solvents (water, ethanol, methanol) with Spartan'14 in References [24,25] in order to illustrate the changes in the spectral characteristics of these solvents and to compare the results with the experimental ones obtained in electronic visible spectra. In References [24, 25], the ternary solutions of the type of ylid + water + alcohol were studied by spectral means in order to evaluate the influence of the specific interactions between ylid and hydroxyl molecules. The small differences between the interaction energies in the molecular pairs of ylid–alcohol and ylid–water showed that the hydroxyl molecules can participate in specific interactions with the basic ylids. In this study, DMF was chosen because it solves the studied ylids and cannot participate in specific interactions with the ylid molecules, with DMF having the acidity parameter $\alpha = 0$ and the basicity parameter $\beta = 0$. So, the spectral shifts in DMF are affected only by the universal interactions.

The aim of this study was to compare the computational results obtained for four carbanion monosubstituted 4'-aryl-1,2,4-triazol-1-ium-4-R₂-phenacylid molecules in the gaseous phase (isolated molecules) and in DMF.

The 1,2,4-triazol-1-ium phenacylids are soluble in a few organic solvents. Their reduced solubility in most solvents does not allow solvatochromic studies to obtain some molecular parameters in the electronic states responsible for the light absorption process [5,24,25].

Dimethylformamide, a polar, hydrophilic, colorless and odorless liquid, was chosen for this study. Some computational and spectral results obtained for the studied 4'-aryl-1,2,4-triazol-1-ium-4-R₂-phenacylid molecules in water and alcohol, in which the ylid molecules participate in specific interactions (by hydrogen bond formation), were previously published [24,25].

DMF is an aprotic liquid in which ylids do not participate in specific interactions. The global quantum chemical descriptors characterizing the chemical properties of the ylids were computed and compared with those of the corresponding derivatives.

The results reported here can help chemists to establish new procedures for obtaining new heterocycles used in a great number of pharmaceutical and industrial applications.

2. Computational and Experimental Details

The quantum mechanical analysis of the studied methylids was performed with the Spartan'14 program [26,27] using the EDF2/6-31G* density functional method (DFT) described in [28]. The EDF2 method was used since it was constructed to yield accurate

harmonic vibrational frequencies, but it appears also to afford accurate structures and thermochemistry data.

The electronically excited states were calculated by optimizing the geometry of the molecules in the excited states using the time-dependent DFT (TDDFT) algorithm.

The data related to the solvation in DMF were obtained by using the semi-empirical model SM8, under the Spartan'14 program.

The substances were prepared as described in [18–20], and their purity was established by spectral (FTIR and NMR) and chemical (elemental) analyses. ^1H NMR spectra (DMSO- d_6 , 400 MHz) were recorded using a Bruker ARX 400 spectrometer, while the FTIR spectra were recorded with a Specord NIR 71 Carl Zeiss Jena spectrophotometer in KI.

The electronic absorption spectra of the diluted (10^{-4} mol/L) solutions of 4'-aryl-1,2,4-triazol-1-ium-4- R_2 -phenacylids in DMF were recorded with Specord UV Vis spectrophotometer Carl Zeiss Jena with a data acquisition system.

DMF for spectral analyses was purchased from Merck and used without purification.

3. Results and Discussions

The chemical structure of the studied carbanion monosubstituted 4'-aryl-1,2,4-triazol-1-ium-4- R_2 -phenacylids is schematically specified in Figure 1.

- (1) $R_1 = R_2 = \text{H}$: 4'-phenyl-1,2,4-triazol-1-ium-phenacylid (PTPY)
- (2) $R_1 = \text{CH}_3$, $R_2 = \text{H}$: 4'-tolyl-1,2,4-triazol-1-ium-phenacylid (TTPY)
- (3) $R_1 = \text{H}$, $R_2 = \text{Cl}$: 4'-phenyl-1,2,4-triazol-1-ium-4-chloro-phenacylid (PTCIPY)
- (4) $R_1 = \text{CH}_3$, $R_2 = \text{Cl}$: 4'-tolyl-1,2,4-triazol-1-ium-4-chloro-phenacylid (TTCIPY)

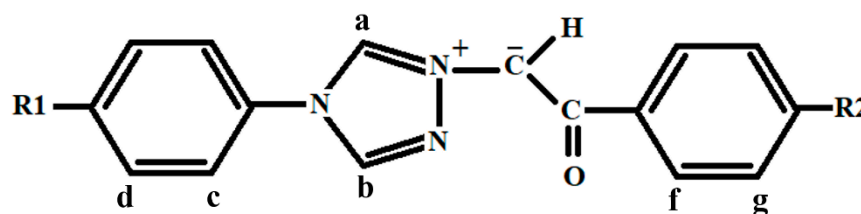


Figure 1. Schematic formula of the studied 4'-aryl-1,2,4-triazol-1-ium-4- R_2 -phenacylid. The lower-case letters (a, b, c, d, f and g) indicate the positions of the protons for which the ^1H NMR spectral data are given in Table 1.

Table 1. Data related to the ^1H NMR (δ in ppm for the protons in the positions specified in Figure 1) and FTIR (frequency of the C=O valence band) spectra.

	δ (ppm)						$\nu_{\text{C=O}}$
	H_a	H_b	H_c	H_d	H_f	H_g	(cm^{-1})
PTPY	11.05	9.46	7.20	7.41	7.62	7.35	1540
TTPY	11.15	9.28	7.08	7.17	7.71	7.38	1550
PTCIPY	11.23	9.11	7.24	7.39	7.91	7.23	1545
TTCIPY	11.27	9.22	7.35	7.44	7.85	7.16	1540
D1	10.94	10.94	7.28	7.50	7.96	7.68	1575
D2	11.21	11.21	7.34	7.37	7.79	7.54	1580
D3	11.10	11.10	7.50	7.64	8.14	7.60	1590
D4	11.16	11.16	7.54	7.62	8.02	7.58	1580

The corresponding symmetric derivatives, used for comparison in our study, are schematically drawn in Figure 2.

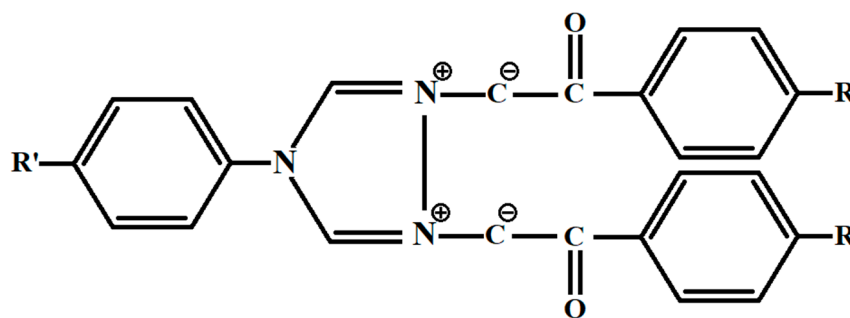


Figure 2. Schematic formula of symmetric substituted compounds corresponding to the studied 4'-aryl-1,2,4-triazol-1-ium-4-R₂-phenacylids.

(D1) R' = H, R = H, (D2) R' = CH₃, R = H, (D3) R' = H, R = Cl, (D4) R' = CH₃, R = Cl.

The symmetric substituted 1,2,4-triazolium ylid derivatives attributed to the C_{2v} point group of symmetry and corresponding to the compounds from Figure 1 are schematically drawn in Figure 2. These molecules possess four elements of symmetry: the plane of the molecule, the plane perpendicular to the molecular plane, one axis of the second order at the intersection of the symmetry planes and the identity. All symmetry operations relative to these elements (reflection in plane, rotation with 180 degrees around the axis of the second order and the identity) transform the compound in itself.

4'-Phenyl-1,2,4-triazol-1-ium (PTPY) and 4'-Tolyl-1,2,4-triazol-1-ium (TTPY) phenacylids are carbanion monosubstituted methylids with a phenyl and a tolyl cycle, respectively, substituted to the triazolium ring in the para position, and having the phenacyl group covalently bonded to their carbanion. In PTCIPY and TTCIPY, the hydrogen from the para position of PTPY and TTPY phenacyl, respectively, is substituted by a chlorine atom.

The data related to the ¹H NMR and FTIR spectra are shown in Table 1.

The electronic spectra and the computed parameters in vacuum, water and ethanol of 4'-aryl-1,2,4-triazol-1-ium-4-R₂-phenacylids were studied and previously published [24,25]. The basic nature of these molecules and their ability to interact with protic solvents by hydrogen bonds were emphasized in the previously published articles. The studied molecules cannot participate in specific interactions with DMF due to their aprotic nature.

Now, we compare the physical properties of these phenacylids in vacuum and DMF, using the results obtained in calculations with the Spartan'14 program. The obtained data are listed in Tables 2 and 3. They are used to characterize the studied molecules from the point of view of their stability, reactivity, polarity or ability to pass through the cell membranes.

The absolute values of the molecular energy (see Tables 2 and 3) of all studied ylids increase in DMF, indicating the increase in their stability compared to the vacuum state.

The frontier orbitals have an important role in determining the ionization potential, electron affinity, chemical reactivity, spectroscopic excitation energy and so on.

According to Koopmans' theorem [29], the ionization potential (*I*) and the electron affinity (*A*) can be calculated from Equations (1) and (2):

$$I = -E_{HOMO} \quad (1)$$

$$A = -E_{LUMO} \quad (2)$$

The potential gap (3) informs about the lowest energy necessary for electronic excitation.

$$\Delta E = |E_{HOMO} - E_{LUMO}| \quad (3)$$

The reactivity of the molecules can also be characterized by the distance between the HOMO and LUMO computed using relation (3). The small values of ΔE indicate that the molecules have high chemical reactivity. The small values of the energy gap (computed with data from Tables 2 and 3) indicate a molecular structure with appreciable polarizability.

and small values of the excitation energy. The values of ΔE are in the visible range and indicate the possibility of all studied carbanion monosubstituted p-R₁-1,2,4-triazol-1-ium-4-R₂-phenacylids to absorb visible photons.

Table 2. Molecular properties of PTPY and TTPY in vacuum and in DMF solution.

	PTPY		TTPY	
	Vacuum	DMF	Vacuum	DMF
Formula	C ₁₆ H ₁₃ N ₃ O	C ₁₆ H ₁₃ N ₃ O	C ₁₇ H ₁₅ N ₃ O	C ₁₇ H ₁₅ N ₃ O
Weight (amu)	263.300	263.300	277.327	277.327
Energy (au)	−856.338	−856.375	−895.598	−895.658
Solvation E (kJ/mol)		−97.12		−157.50
E HOMO (eV)	−4.52	−4.73	−4.35	−4.72
E LUMO (eV)	−1.43	−1.18	−1.46	−1.16
Dipole Moment (D)	7.14	10.24	10.54	10.79
Conformers	6	6	6	6
Area (Å ²)	290.87	291.46	314.64	311.37
Volume (Å ³)	275.96	276.19	295.33	294.40
PSA (Å ²)	23.370	23.730	25.017	23.730
Ovality	1.42	1.42	1.47	1.45
Polarizability (Å ³)	63.03	62.94	64.65	64.41
HBD Count	0	0	0	0
HBA Count	3	3	3	3

Table 3. Molecular properties of PTCIPY and TTCIPY in vacuum and in DMF solution.

	PTCIPY		TTCIPY	
	Vacuum	DMF	Vacuum	DMF
Formula	C ₁₆ H ₁₂ ClN ₃ O	C ₁₆ H ₁₂ ClN ₃ O	C ₁₇ H ₁₄ ClN ₃ O	C ₁₇ H ₁₄ ClN ₃ O
Weight (amu)	297.745	297.745	311.772	311.772
Energy (au)	−1315.965	−1316.001	−1355.249	−1355.285
Solvation E (KJ/mol)		−94.50		−94.50
E HOMO (eV)	−4.68	−4.77	−4.63	−4.75
E LUMO (eV)	−1.53	−1.24	−1.44	−1.22
Dipole Moment (D)	9.57	12.80	10.16	13.30
Conformers	4	4	4	4
Area (Å ²)	306.55	307.14	326.46	327.13
Volume (Å ³)	289.63	289.85	307.85	308.08
PSA (Å ²)	23.355	23.746	23.323	23.780
Ovality	1.45	1.45	1.48	1.48
Polarizability (Å ³)	64.12	64.05	65.59	65.53
HBD Count	0	0	0	0
HBA Count	3	3	3	3

The polar surface area (PSA) is used for the prediction of transport properties [30]. PSA values of less than 90 Å² demonstrate that the studied molecules penetrate the blood–brain barrier and can pass through the cell membranes in given conditions [31]. Therefore, these molecules could be used for pharmaceutical purposes.

The absolute values of the HOMO level are higher in DMF compared with vacuum. Therefore, the stability of the studied phenacylids in their ground electronic state is higher in DMF compared with that of the isolated molecules. The LUMO level of PTPY, TTPY, PTCIPY and TTCIPY is destabilized in DMF compared with the isolated molecules, as it results from the values of this orbital energy listed in Tables 2 and 3. In the electronic excited state, the studied molecules have lower stability in the DMF solution compared with the vacuum state.

From the data shown in Tables 2 and 3, one can conclude that the reactivity of the phenacylids PTPY, TTPY, PTCIPY and TTCIPY is higher for their isolated molecules com-

pared to those solved in DMF because the difference ΔE is smaller in their isolated state than in solution. The ground-state dipole moment of all studied molecules increases in the solvation process, while the ground-state electric polarizability is not significantly modified in DMF, compared to the gaseous state.

PSA parameter increases for all studied molecules by solvation in DMF, compared to the gaseous phase. The values of PSA both in vacuum and in DMF are not higher than 25 \AA^2 for all studied phenacylids. These values of PSA show that, in given conditions, the studied ylids can penetrate the cell membranes and can pass through the blood–brain barrier [30]. It confirms the possibility to utilize the studied phenacylids in the drug industry [32].

As it results from Tables 2 and 3, the difference ΔE (computed using relation (3)) increases in the solvation process for all molecules, indicating the shift to blue of the visible electronic band which appears by electron transitions between HOMO and LUMO levels when the studied molecules pass from the vacuum in solutions.

The studied ylids have a basic character: they can add protons in three zones (HBA = 3), according to data from Tables 2 and 3.

In Table 4, some molecular descriptors are given, computed using the data in Tables 2 and 3 for the studied carbanion monosubstituted 4'-aryl-1,2,4-triazol-1-ium-4-R₂-phenacylids and for their derivatives with the highest symmetry. The global quantum molecular descriptors from Table 4 are defined as follows [30,33]:

$$\text{Chemical hardness } \eta = \frac{I - A}{2} \quad (4)$$

$$\text{Electronegativity } \chi = \frac{I + A}{2} \quad (5)$$

$$\text{Electrophilicity index } \omega = \frac{\chi^2}{2\eta} \quad (6)$$

$$\text{Chemical potential } \mu = -\chi \quad (7)$$

$$\text{Softness } S = \frac{1}{\eta}. \quad (8)$$

Table 4. Some molecular descriptors for studied 4'-aryl-1,2,4-triazol-1-ium phenacylids, 4'-aryl-1,2,4-triazol-1-ium-p-chloro-phenacylids and for their derivatives.

	<i>I</i> (eV)	<i>A</i> (eV)	η (eV)	χ (eV)	ω (eV)	μ (eV)	<i>S</i> (eV ^{−1})
PTPY	4.52	1.53	1.495	3.025	3.060	−3.025	0.669
D1	5.13	1.96	1.585	3.545	3.964	−3.545	0.631
TTPY	4.35	1.46	1.445	2.905	2.920	−2.905	0.692
D2	5.07	1.89	1.590	3.480	3.808	−3.480	0.629
PTCPY	4.68	1.53	1.575	3.105	3.061	−3.105	0.635
D3	5.36	2.13	1.615	3.745	4.342	−3.745	0.619
TTCPY	4.63	1.44	1.595	3.035	2.890	−3.035	0.692
D4	5.30	2.01	1.645	3.480	4.060	−3.655	0.629

The symmetrically substituted derivatives (D1–D4) of the carbanion monosubstituted 4'-aryl-1,2,4-triazol-1-ium-4-R₂-phenacylids are characterized by higher values of the ionization potential, electron affinity, chemical hardness and electrophilicity index compared with their corresponding ylids. This fact shows that the carbanion monosubstituted 4'-aryl-1,2,4-triazol-1-ium-4-R₂-phenacylids are characterized by a higher reactivity compared with their symmetric derivatives. The chemical hardness of the derivatives D1–D4 is probably due to their complexity and also to the symmetrical substitution which induces the symbiosis effect [34–36]. Moreover, the existing positive and negative charges of symmetric derivatives tend to induce canceling effects (like in a tug-of-war game) leading to a higher stability of these molecules.

The molecular descriptors are very important in organic chemistry both for information about the molecular chemical reactivity and for the possibility to recognize the presence of impurities in a mixture [37–39].

The electrostatic charges near the atoms in the studied molecules, calculated with Spartan'14, are listed in Figures 3 and 4 for vacuum and DMF solutions, respectively. The arrow indicate the direction of the molecule's electric dipole moment. The values of the electrostatic charges near the atoms of the ylid bond and also near the carbonyl atomic group, calculated with Spartan'14, are listed in Table 5.

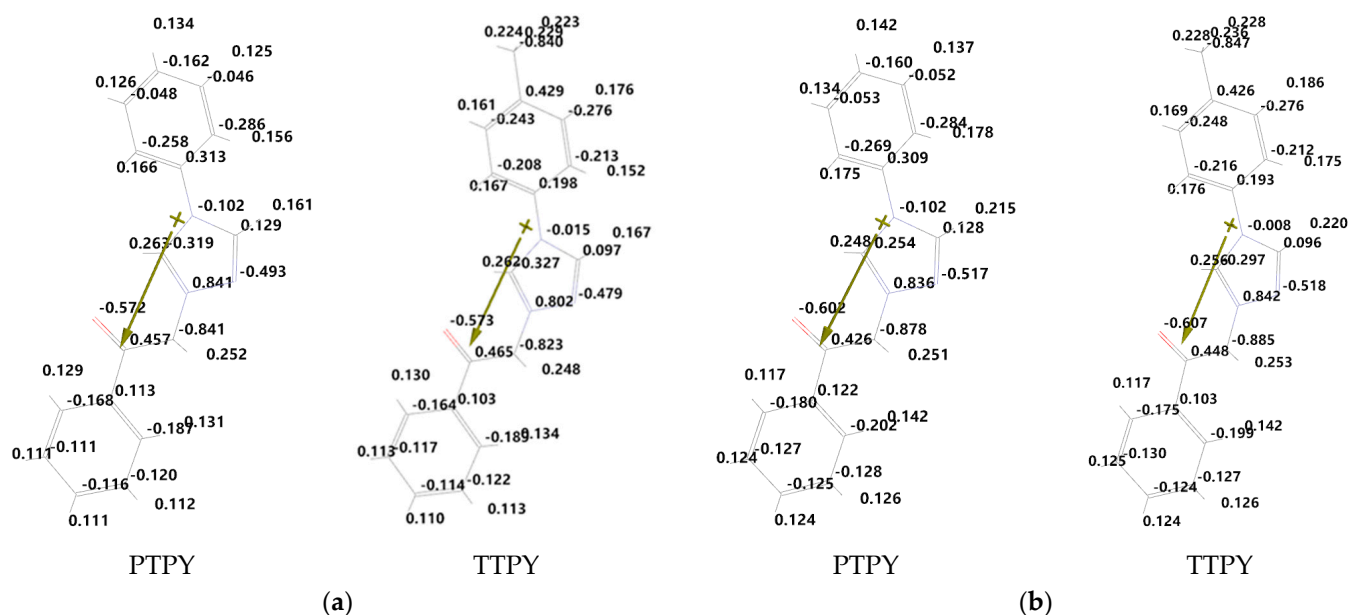


Figure 3. Electrostatic charges (expressed in electronic charges) near the molecular atoms, calculated with Spartan'14 in (a) vacuum state and (b) DMF solution for PTPY and TTPY phenacylids.

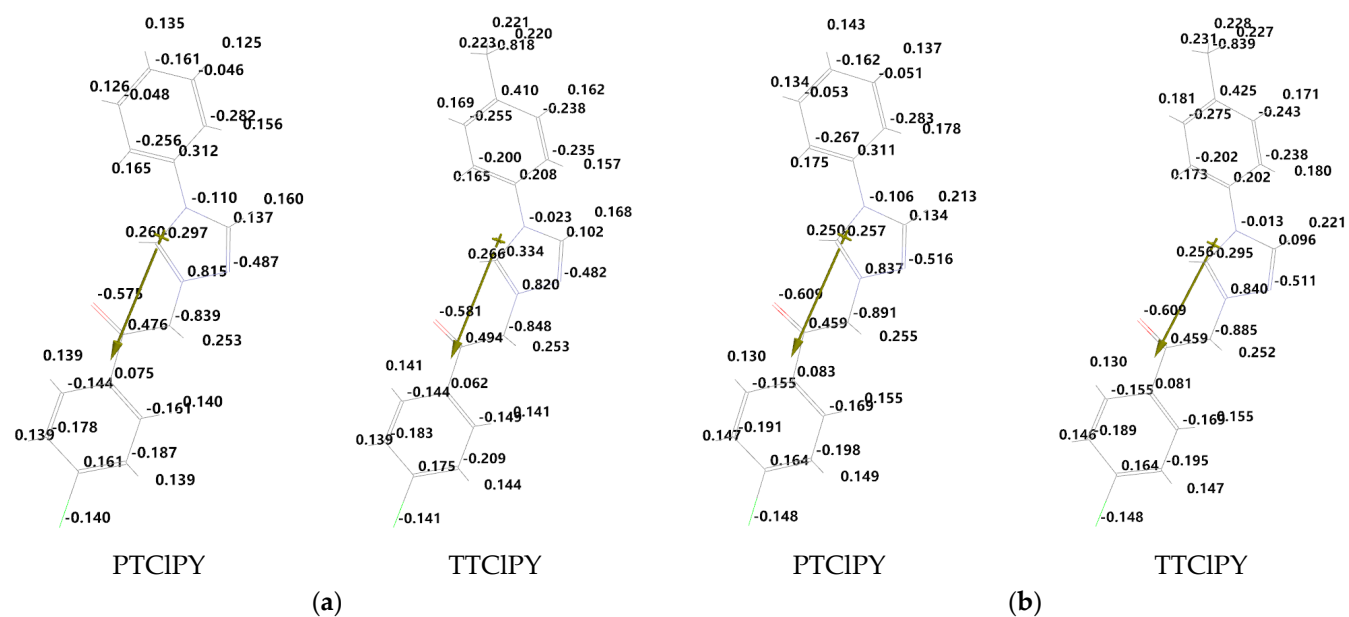


Figure 4. Electrostatic charges (expressed in electronic charges) near the molecular atoms, calculated with Spartan'14 in (a) vacuum state and (b) DMF solution for PTCIPY and TTCIPY phenacylids.

Table 5. Electrostatic charges (expressed in electronic charges) near the ylid bond (N^+-C^-) and on the atoms of $C=O$, calculated with Spartan'14.

	PTPY		TTPY		PTCIPY		TTCIPY	
	Vacuum	DMF	Vacuum	DMF	Vacuum	DMF	Vacuum	DMF
N^+	0.841	0.836	0.802	0.842	0.815	0.837	0.820	0.840
C^-	−0.841	−0.878	−0.823	−0.855	−0.839	−0.891	−0.848	−0.885
C	0.457	0.426	0.465	0.448	0.476	0.459	0.494	0.459
O	−0.572	−0.602	−0.573	−0.607	−0.575	−0.605	−0.581	−0.609

The data in Figures 3 and 4 and Table 5 suggest that, by solvation in DMF, there are modifications in the polarity of the ylid bond and also in the carbonyl atomic group. These atomic groups are of interest because specific interactions can act at their levels.

The changes in the electronic charge distribution on the molecular atoms can modify the value and the orientation of the molecular dipole moment. The data in Tables 2 and 3 suggest that, by solvation in DMF, the electric dipole moment of all studied phenacylids increases.

The values of HOMO and LUMO levels, computed with Spartan'14 for the studied ylids in vacuum and in DMF (presented in Tables 2 and 3), show that for the isolated molecules, in vacuum, by substituting a hydrogen atom in the benzene ring of the phenacyl with a chlorine atom, the distance between the electronic levels of the HOMO and LUMO increases.

The computed distance between HOMO and LUMO levels also increases when the studied molecules pass from the isolated state to the DMF solution.

The wavenumbers (expressed in cm^{-1}) in the maximum of the visible electronic absorption band measured in DMF are compared with the computed difference between the HOMO and LUMO in DMF. The increase in the wavenumbers of the visible band for all studied ylids (see Figure 5) (measured in the maximum of the electronic absorption spectrum of their diluted solutions in DMF), compared with the computed ones for isolated molecules (in vacuum), results from the data in Table 6 and shows a higher stabilization of the fundamental level of the electronic transition compared with the excited state of all phenacylids under study.

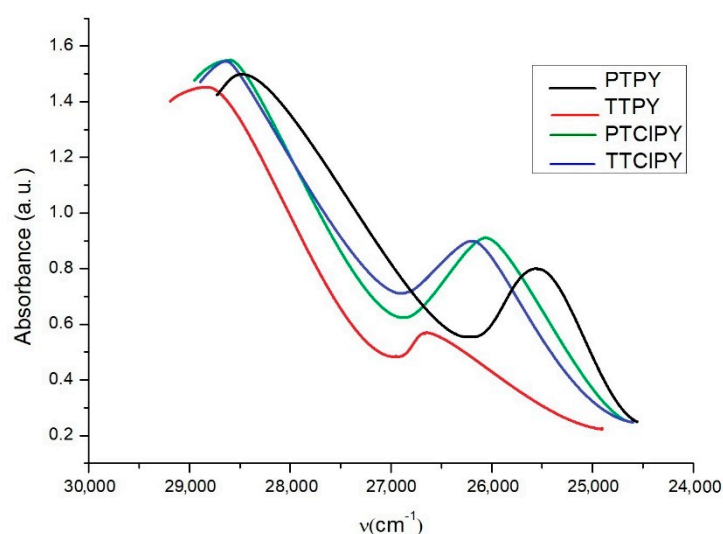
**Figure 5.** Visible electronic bands of the studied 4'-aryl-1,2,4-triazol-1-ium-4-R₂-phenacylids, recorded in DMF.

Table 6. Wavenumbers (cm^{-1}) in the maximum of the visible absorption bands recorded in DMF; the computed values of ΔE (in cm^{-1}) in vacuum and DMF and the dipole moments in the ground states for the studied 4'-aryl-1,2,4-triazol-1-ium-4- R_2 -phenacylids.

Phenacylid	ν_{exp}	ΔE_{vacuum}	ΔE_{DMF}	$\mu_g(\text{D})$
PTPY	25,550; 28,470	24,924	28,634	7.14
TTPY	26,660; 28,810	23,311	28,715	10.54
PTCIPY	26,060; 28,850	25,408	28,473	9.57
TTCIPY	26,200; 28,620	25,731	28,473	10.16

Relations of type (9) can be established [24,25] to describe the universal interactions of the orientation–induction and dispersion types, respectively.

$$h\nu r^3 = A\mu_g^2 + B\mu_g + C. \quad (9)$$

In relation (9), $h\nu$ is the energy expressed in erg, r is the Onsager radius of the spectrally active molecule, μ_g is the computed dipole moment of the solute molecule in the ground state for its gaseous phase (see Tables 2 and 3), while A , B and C are regression coefficients depending on the molecular parameters.

A dependence of the product $h\nu r^3$ vs. the ground-state dipole moment of the studied molecules described by relation (9) can be established for both visible electronic bands recorded in DMF, as results from Figure 6.

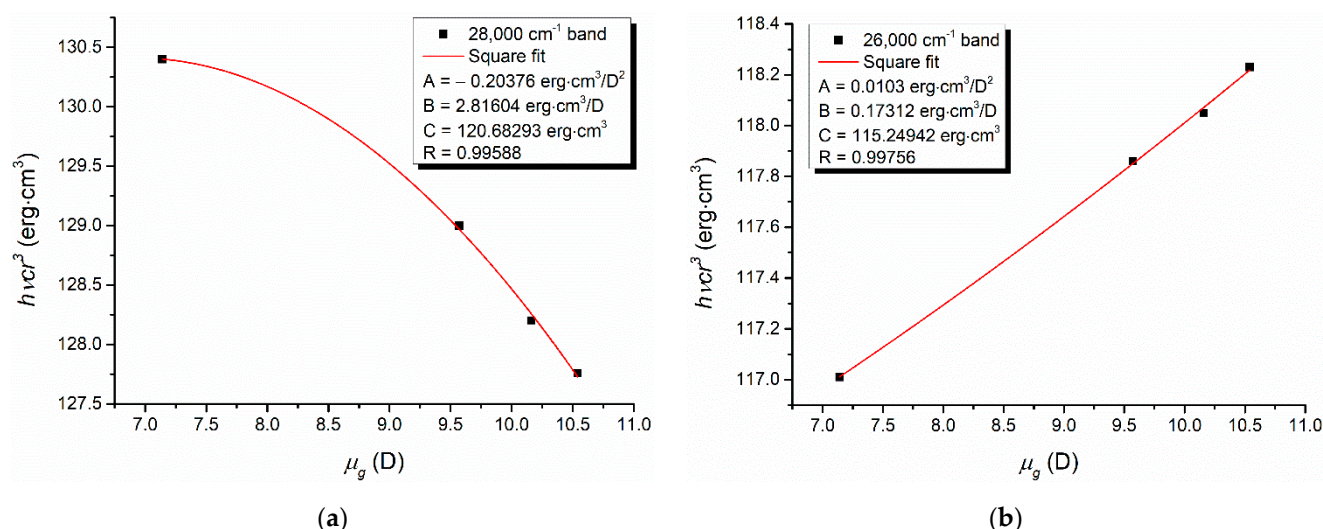


Figure 6. $h\nu r^3$ vs. μ_g for 28,000 cm^{-1} (a) and 26,000 cm^{-1} (b) bands, respectively. The red line corresponds to the fitting of the points according to Equation (9) (the inset panels contain the regression coefficients A , B and C , as well as the correlation coefficient R).

The dependences illustrated in Figure 6 confirm that in the DMF solutions, the universal interactions (orientation, induction and dispersion) act between the spectrally active and solvent molecules. Since $\text{HBD} = 0$ for all the studied ylids and $\alpha = 0$ (Kamlet–Taft parameter modeling the hydrogen bond donation ability [40]) for DMF, specific interaction with the formation of a hydrogen bond is impossible in the studied solutions.

The HOHO and LUMO maps of the studied molecules are illustrated in Figure 7 for the isolated molecules and in Figure 8 for their solution in DMF, respectively.

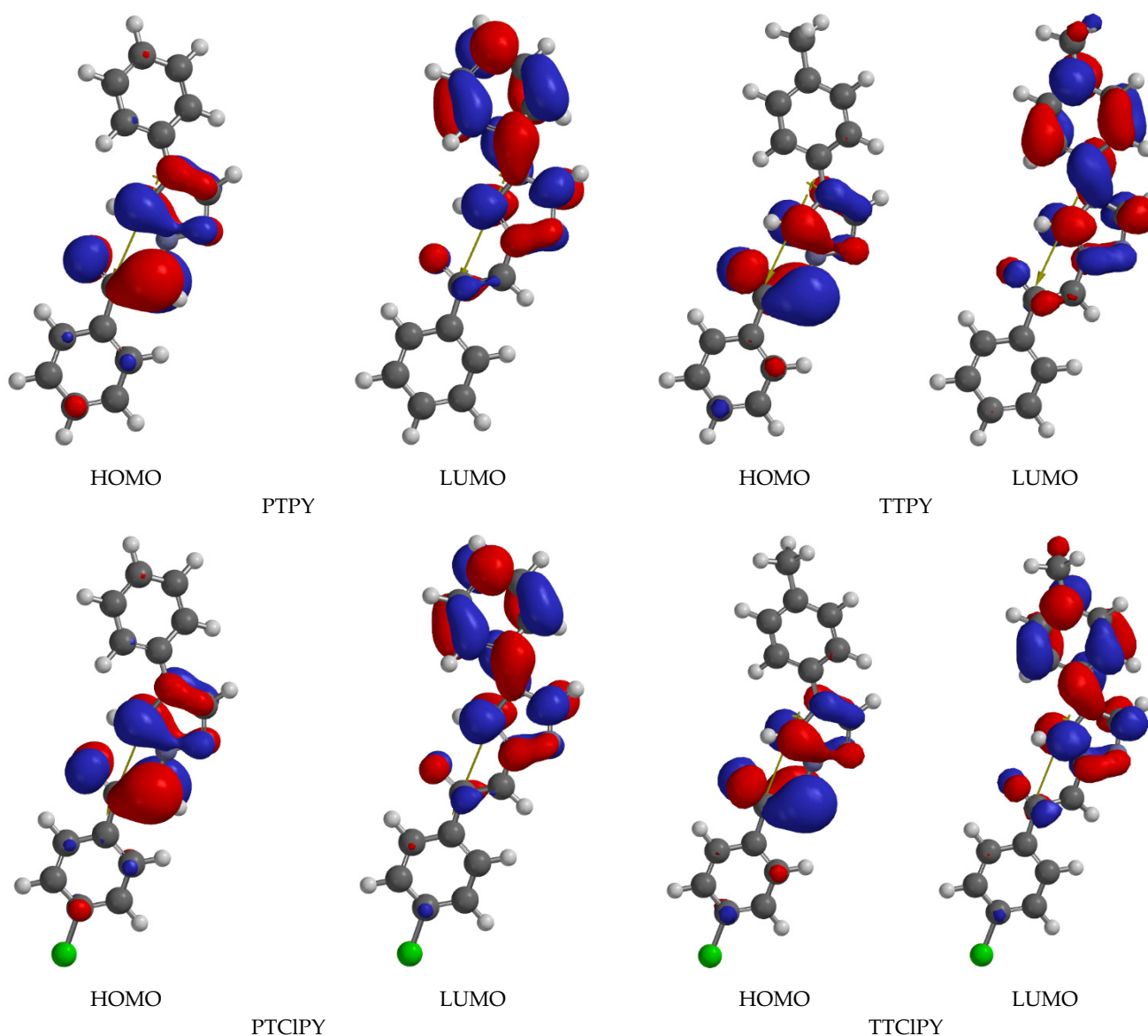


Figure 7. HOMO and LUMO maps in vacuum phase of the studied ylids.

Figure 7 shows important changes in the symmetry of the valence electron density when the molecules pass from their ground electronic state to the excited state.

As depicted in Figure 7, the computations show that the electronic charges for all studied phenacylids in the HOMO have similar distributions in the vacuum phase. LUMO maps of PTPY, TTPY, PTCIPY and TTCIPY show an increase in electron density on the aryl substituent of the heterocycle in the vacuum state, as was indicated in [18–20]. This observation is important when the visible band of these phenacylids is attributed to one electronic absorption transition and also to explain the spectral shifts recorded in their visible electronic absorption spectra.

For the vacuum state of PTPY, TTPY, PTCIPY and TTCIPY, the charge transfer is realized from the carbanion toward the heterocycle and its substituent, as has been established previously [18–20].

Figure 8 shows that the HOMO maps are similar for all studied phenacylids, indicating the higher electron density on the triazolium ring and on the atomic group C=O. It also shows the similarity of the LUMO maps indicating the spread of the electron density on the entire molecule for all studied phenacylids in their excited states. This conclusion shows

that in DMF, the electronic absorption band appears by a transition that determines the valence electron cloud spreading on the entire molecular skeleton [24,25].

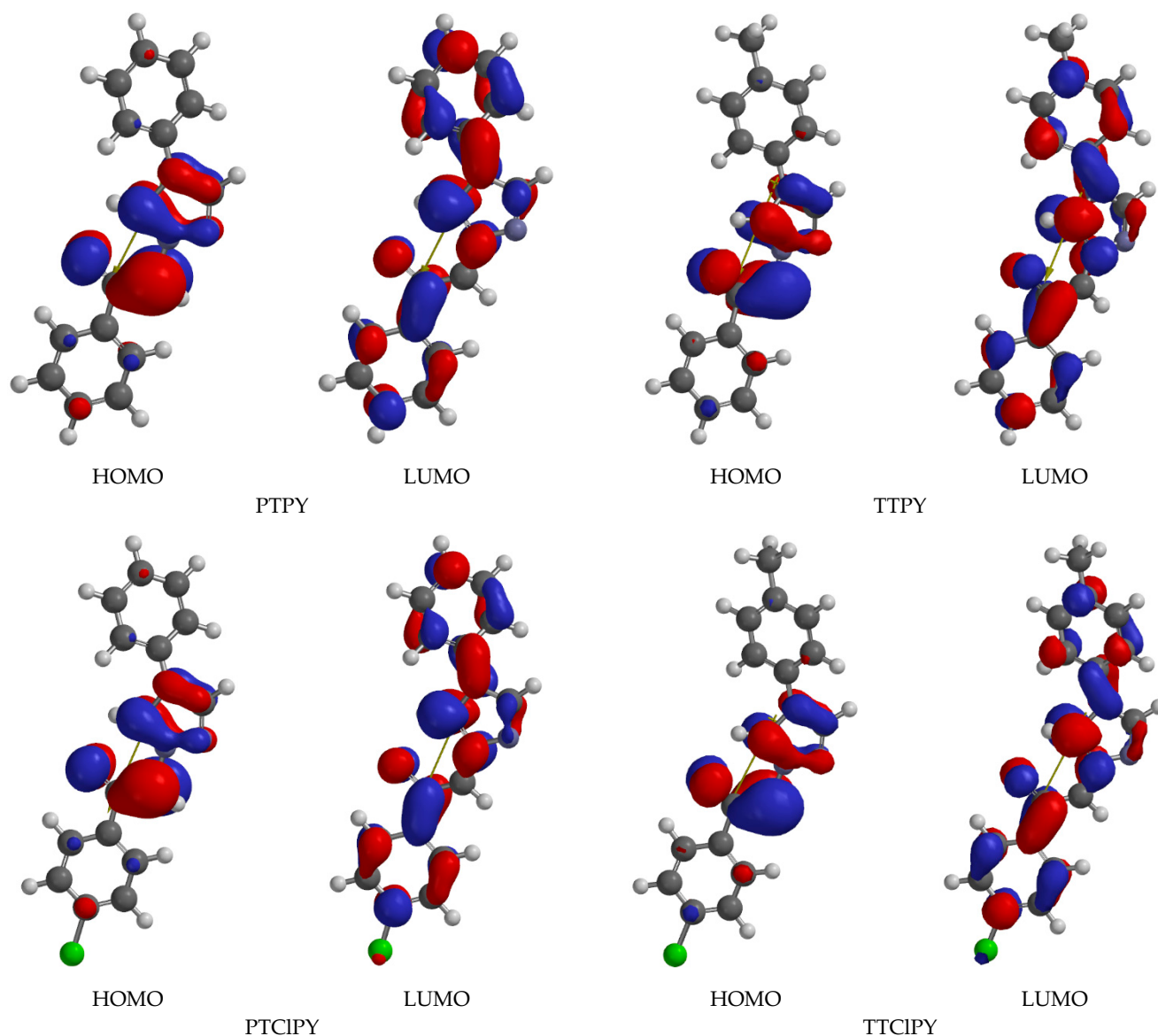


Figure 8. HOMO and LUMO maps in DMF solution of the studied ylids.

The energy of the intermolecular interactions between the ylid molecules and the DMF molecules is proportional to the difference between the distances HOMO–LUMO in DMF and in vacuum. When the p-hydrogen from phenyl is substituted by the atomic group $-\text{CH}_3$, the spectral shift measured in DMF relative to vacuum increases in PTPY and TTPY molecules and decreases in the pairs PTCIPY and TTCIPY, respectively.

This study demonstrates the difference between the electronic transition natures responsible for the visible absorption band appearance in vacuum and in DMF for all studied ylids.

The influence of the DMF on the chemical reactivity and spectral properties of the studied ylids is underlined in this study. Some molecular descriptors calculated based on the HOMO and LUMO energies of the studied compounds are also compared with those computed for the corresponding symmetrically substituted derivatives.

4. Conclusions

The parameters of the studied 4'-aryl-1,2,4-triazol-1-ium-p-R₂-phenacylids computed with the Spartan'14 program show that these molecules are dipolar and their dipole moment in the ground electronic state increases when they are dissolved in DMF relative to the isolated molecules.

All studied phenacylids can be excited by visible photons. Due to the reduced interval between the HOMO and LUMO (ΔE), these molecules have a high photoreactivity.

The PSA values show that the phenacylid molecules under study can penetrate, in given conditions, the cell membranes and can pass through the blood–brain barrier, indicating the possibility of their use in the drug industry.

The quantum mechanical modeling shows modifications in the polarity of the ylid bond and an increase in the polarity in the carbonyl group.

The HOMO and LUMO maps demonstrate the difference between the distribution of the valence electrons (charge transfer) in the excited state of the studied ylids in both vacuum and DMF.

By using some derivatives with a high degree of symmetry, one can show that the carbanion monosubstituted 4'-aryl-1,2,4-triazol-1-ium-p-R₂-phenacylids are indicated for chemical reactions for obtaining new heterocyclic compounds, having a higher chemical reactivity than their corresponding derivatives.

Author Contributions: Conceptualization, D.-O.D. and D.-G.D.; methodology, N.M.P.; software, D.-G.D., G.A. and A.C.M.; validation, N.M.P., D.-G.D. and D.-O.D.; formal analysis, G.A. and A.C.M.; investigation, G.A.; resources, N.M.P.; data curation, N.M.P.; writing—original draft preparation, D.-O.D.; writing—review and editing, N.M.P.; visualization, D.-G.D.; supervision, D.-O.D. and D.-G.D.; project administration, N.M.P.; funding acquisition, N.M.P. All authors have read and agreed to the published version of the manuscript.

Funding: Authors are thankful to the Romanian Ministry of Research, Innovation and Digitization, within Program 1—Development of the national RD system, Subprogram 1.2—Institutional Performance—RDI excellence funding projects, Contract no. 11PFE/30.12.2021, for financial support.

Data Availability Statement: The data presented in this study are available on request from the corresponding author.

Conflicts of Interest: The authors declare no conflict of interest.

References

1. Lars-Flörl, C. Triazole antifungal agents in invasive fungal infections: A comparative review. *Drugs* **2011**, *71*, 2405–2411. [[CrossRef](#)] [[PubMed](#)]
2. Sathish Kumar, S.; Kavitha, H.P. Synthesis and biological applications of triazole derivatives—A review. *Mini Rev. Org. Chem.* **2013**, *10*, 40–65. [[CrossRef](#)]
3. Zhang, F.-F.; Gan, L.-L.; Zhou, C.-H. Synthesis, antibacterial and antifungal activities of some carbazole derivatives. *Bioorg. Med. Chem. Lett.* **2010**, *20*, 1881–1884. [[CrossRef](#)] [[PubMed](#)]
4. Al-Omar, M.A.; Al-Abdullah, E.S.; Shehata, I.A.; Habib, E.E.; Ibrahim, T.M.; El-Emam, A.A. Synthesis, antimicrobial and anti-inflammatory activities of novel 5-(1-adamantyl)-4-aryldeneamino-3-mercapto-1,2,4-triazoles and related derivatives. *Molecules* **2010**, *15*, 2526–2550. [[CrossRef](#)] [[PubMed](#)]
5. Closca, V.; Melniciuc-Puica, N.; Benchea, A.C.; Dorohoi, D.O. Intermolecular interactions in ternary solutions of some 1,2,4-triazolium ylids studied by spectral means. *Proc. SPIE* **2014**, 9286, 92862T. [[CrossRef](#)]
6. Huang, R.-Z.; Liang, G.-B.; Li, M.-S.; Fang, Y.-L.; Zhao, S.-F.; Zhou, M.-M.; Liao, Z.-X.; Sun, J.; Wang, H.-S. Synthesis and Discovery of asiatic acid based 1,2,3-triazole derivatives as antitumor agents blocking NF- κ B activation and cell migration. *MedChemComm* **2019**, *10*, 584–597. [[CrossRef](#)]
7. Yang, J.-J.; Yu, W.-W.; Hu, L.-L.; Liu, W.-J.; Lin, X.-H.; Wang, W.; Zhang, Q.; Wang, P.-L.; Tang, S.-W.; Wang, X.; et al. Discovery and characterization of 1H-1,2,3-triazole derivatives as novel prostanoid EP4 receptor antagonists for cancer immunotherapy. *J. Med. Chem.* **2020**, *63*, 569–590. [[CrossRef](#)]
8. Singh, D.; Panigrahi, S.K.; Sharma, G.; Gardas, R.L. Scrutinizing the stability of haemoglobin in 1,2,4-triazolium based ionic liquid. *J. Mol. Liq.* **2021**, *349*, 118213. [[CrossRef](#)]
9. Riccobono, A.; Lazzara, G.; Rogers, S.E.; Pibiri, I.; Pace, A.; Slattery, J.M.; Bruce, D.W. Synthesis and mesomorphism of related series of triphilic ionic liquid crystals based on 1,2,4-triazolium cations. *J. Mol. Liq.* **2021**, *321*, 114758. [[CrossRef](#)]

10. Paramparambath, S.; Selvam, S.; Puthukkudy, G.; Satheesh, A.; Kandasamy, E. An efficient strategy to synthesis of β -carbonyl compounds by 1-pentyl-1,2,4-triazolium methanesulfonate. *Mater. Today Proc.* **2020**, *33*, 2144–2147. [CrossRef]
11. Gayathri, K.M.; Paramparambath, S.; Satheesh, A.; Selvam, S.; Kandasamy, E. Reduction of aldehydes and ketones by NaBH_4 in presence of 1-alkyl-1,2,4-triazolium salts. *Mater. Today Proc.* **2020**, *33*, 2381–2384. [CrossRef]
12. Castells, J.; Geijo, F.; López-Calahorra, F. The “formoin reaction”: A promising entry to carbohydrates from formaldehyde. *Tetrahedron Lett.* **1980**, *21*, 4517–4520. [CrossRef]
13. Teles, J.H.; Melder, J.-P.; Gehrler, E.; Harder, W.; Ebel, K.; Groening, C.; Meyer, R. Addition Products of Triazolium Salts. U.S. Patent 5508422, 16 April 1996.
14. Karczmarzyk, Z.; Swatko-Ossor, M.; Wysocki, W.; Drozd, M.; Ginalska, G.; Pachuta-Stec, A.; Pitucha, M. New applications of 1,2,4-triazole derivatives as antitubercular agents. Structure, in vitro screening and docking studies. *Molecules* **2020**, *25*, 6033. [CrossRef] [PubMed]
15. Chu, X.-M.; Wang, C.; Wang, W.-L.; Liang, L.-L.; Liu, W.; Gong, K.-K.; Sun, K.-L. Triazole derivatives and their antiplasmodial and antimalarial activities. *Eur. J. Med. Chem.* **2019**, *166*, 206–223. [CrossRef] [PubMed]
16. Alrawashdeh, M.S.M. Determination of antimicrobial activity of some 1,2,4-triazole derivatives. *Regul. Mech. Biosyst.* **2018**, *9*, 203–208. [CrossRef]
17. Borowiecki, P.; Milner-Krawczyk, M.; Pleniewicz, J. Chemoenzymatic synthesis and biological evaluation of enantiomerically enriched 1-(β -hydroxypropyl) imidazolium- and triazolium-based ionic liquids. *Beilstein J. Org. Chem.* **2013**, *9*, 516–525. [CrossRef]
18. Zugravescu, I.; Petrovanu, M. *N-Ylid Chemistry*; Academic Press: New York, NY, USA, 1976.
19. Petrovanu, M.; Luchian, C.; Surpateanu, G.; Barboiu, V. 1,2,4-Triazolium ylures. I Synthèse and stéréochimie des reactions de cycloaddition aux composés a liaison éthylénique active. *Rev. Roum. Chim.* **1974**, *24*, 733–744.
20. Surpateanu, G.; Caea, N.; Sufletel, L.; Grandclaoudon, P. Synthesis and characterization of new azatriazolium ylids. *Rev. Roum. Chim.* **1995**, *40*, 133–136.
21. Zhang, Q.; Shreeve, J.M. Energetic ionic liquids as explosives and propellant fuels: A new journey of ionic liquid chemistry. *Chem. Rev.* **2014**, *114*, 10527–10574. [CrossRef]
22. Tankov, I.; Yankova, R. Theoretical (density functional theory) studies on the structural, electronic and catalytic properties of the ionic liquid 4-amino-1H-1,2,4-triazolium nitrate. *J. Mol. Liq.* **2018**, *269*, 529–539. [CrossRef]
23. Wilson, N.D.; Wang, Z.; Gung, B.W. How to control the acidity of 1,2,3-triazolium ions: A density functional theory study. *J. Mol. Graph. Model.* **2022**, *112*, 108133. [CrossRef] [PubMed]
24. Dorohoi, D.O.; Dimitriu, D.G.; Morosanu, A.C.; Puica Melniciuc, N.; Hurjui, I.; Miron, M.; Mariciuc, G.G.; Closca, V.; Cheptea, C. Some aryl-1,2,4-triazol-1-ium phenacylids in binary hydroxyl solvent mixtures. Computational and spectral study. *Symmetry* **2021**, *13*, 1656. [CrossRef]
25. Dorohoi, D.O.; Dimitriu, D.G.; Dulcescu-Oprea, M.M.; Morosanu, A.C.; Puica-Melniciuc, N.; Ardelean, E.; Gritco-Todirascu, A.; Cheptea, C. Solvatochromic study of two carbanion monosubstituted 4-tolyl-1,2,4-triazol-1-ium phenacylids in binary hydroxyl solvent mixtures. *Molecules* **2021**, *26*, 3910. [CrossRef] [PubMed]
26. Spartan'14 for Windows, Macintosh and Linux, Tutorial and User's Guide, 10 January 2014. Modeling. Available online: <http://downloads.wavefun.com/Spartan%20T1%20text%20right%2014Manual.pdf> (accessed on 8 July 2022).
27. Hehre, W.J. *A Guide to Molecular Mechanics and Quantum Chemical Calculations*; Wavefunction, Inc.: Irvine, CA, USA, 2003.
28. Lin, C.Y.; George, M.W.; Gill, P.M.W. EDF2: A density functional for predicting molecular vibrational frequencies. *Aust. J. Chem.* **2004**, *57*, 365–370. [CrossRef]
29. Koopmans, T. Über die zuordnung von wellenfunktionen und eigenwerten zu den einzelnen elektronen eines atoms. *Physica* **1934**, *1*, 104–113. [CrossRef]
30. Hitchcock, S.A.; Pennington, L.D. Structure-brain exposure relationships. *J. Med. Chem.* **2006**, *49*, 7559–7583. [CrossRef] [PubMed]
31. Huigol, M.I.; Sriram, V.; Balasubramanian, K. Structure-ability relations for antiepileptic drugs through omega polynomials and topological indices. *Mol. Phys.* **2022**, *120*, e1987542. [CrossRef]
32. Cheptea, C.; Sunel, V.; Ardeshir, S.M.; Morosanu, A.C.; Dorohoi, D.O. Some physico-chemical characteristics of amino-acid derivatives containing rest of 1,2,4-triazole-3,4-di-substituted with potential antitumoral activity. *Mol. Cryst. Liq. Cryst.* **2020**, *697*, 97–107. [CrossRef]
33. Hurjui, I.; Ivan, M.L.; Dorohoi, D.O. Solvent influence on the electronic absorption spectra (EAS) of 1,6-diphenyl-1,3,5-hexatriene (DPH). *Spectrochim. Acta Part A Mol. Biomol. Spectrosc.* **2013**, *102*, 219–225. [CrossRef]
34. Dorohoi, D.O. Spectroscopy of N-ylids. *J. Mol. Struct.* **2004**, *704*, 31–43. [CrossRef]
35. Surpateanu, G.; Dorohoi, D.O.; Zugravescu, I. Group electronegativity determination I. *Sci. Ann. Al. I. Cuza Univ. Iasi Ib Fizica* **1977**, *23*, 99–102.
36. Surpateanu, G.; Dorohoi, D.O.; Zugravescu, I. Group electronegativity determination II. *Sci. Ann. Al. I. Cuza Univ. Iasi Ib Fizica* **1978**, *22*, 35–40.
37. Gosav, S.; Praisler, M.; Dorohoi, D.O.; Popa, G. Structure-activity correlations for illicit amphetamines using ANN and constitutional descriptors. *Talanta* **2006**, *70*, 922–928. [CrossRef] [PubMed]
38. Gosav, S.; Praisler, M.; Dorohoi, D.O.; Popa, G. Automated identification of novel amphetamines using a pure neutral network and neutral networks coupled with principal component analysis. *J. Mol. Struct.* **2005**, *744–747*, 821–825. [CrossRef]

-
39. Gosav, S.; Praisler, M.; Dorohoi, D.O. ANN expert system screening for illicit amphetamines using molecular descriptors. *J. Mol. Struct.* **2007**, *834–836*, 188–194. [[CrossRef](#)]
 40. Taft, R.W.; Kamlet, M.J. The solvatochromic comparison method. 2. The α -scale of solvent hydrogen-bond donor (HBD) acidities. *J. Am. Chem. Soc.* **1976**, *98*, 2886–2894. [[CrossRef](#)]